

# Carbon Dioxide Reduction with Hydrogen in a Continuous Catalytic Monolith Photoreactor

Beenish Tahir , Muhammad Tahir , Nor A. S. Amin\*

Chemical Reaction Engineering Group/ Low Carbon Energy Group, Faculty of Chemical Engineering, Universiti Teknologi Malaysia, 81310 UTM, Skudai, Johor Baharu, Johor, Malaysia.  
 noraishah@cheme.utm.my

Photocatalytic CO<sub>2</sub> reduction with H<sub>2</sub> as a reductant over gold (Au)-doped TiO<sub>2</sub> nanocatalysts in a continuous monolith photoreactor has been investigated. The nanocatalysts were characterized by XRD, SEM, N<sub>2</sub> adsorption-desorption and UV-Visible spectroscopy. Crystalline nanoparticles of anatase phase TiO<sub>2</sub> were obtained in the Au-doped TiO<sub>2</sub> samples. CO was the major product over 0.5 wt. % Au-doped TiO<sub>2</sub> with the yield rate of 12,305 ppm g-catal.<sup>-1</sup> h<sup>-1</sup>, 318 times higher than un-doped TiO<sub>2</sub> catalyst. Significantly higher photoactivity of Au-doped TiO<sub>2</sub> was obviously due to fast electron transfer with hindered recombination rates and larger illuminated surface area inside the monolith channels. The CO production rate was gradually reduced with increasing the space velocity. The stability of the reused catalysts for CO production sustained at cyclic runs. It is evident Au-doped TiO<sub>2</sub> nanocatalyst supported over monolith channels is highly potential for continuous CO<sub>2</sub> photoreduction to CO and hydrocarbons.

## 1. Introduction

Photocatalytic reduction of carbon dioxide (CO<sub>2</sub>) to useful chemicals has grown into an intense area of research owing to global warming and energy crises (Wang et al., 2015). The reduction of CO<sub>2</sub> to CO, CH<sub>4</sub>, HCOOH, HCHO, and CH<sub>3</sub>OH, with water as the reducing agent, has been reported for the first time more than three decades ago (Inoue et al., 1979). The photocatalytic CO<sub>2</sub> reduction with water is a challenging task as H<sub>2</sub>O is a weak reductant and is hardly reducible. However, photoreduction of CO<sub>2</sub> with H<sub>2</sub> through reverse water gas shift (RWGS) reaction is more effective to produce fuels (Tahir et al., 2015). Among the semiconductors materials, TiO<sub>2</sub> is a promising photocatalyst due to numerous advantages such as strong oxidative-reductive potential, cheaper, abundantly available, and chemically/thermally stable (Ruzmanova et al., 2013). However, TiO<sub>2</sub> photoactivity is relatively lower due to the fast recombination rate of electron-holes pairs, which can be improved by modifying its structure with noble metals (Sacco et al., 2015). Among the noble metals, gold (Au) nanoparticles doping into TiO<sub>2</sub> can efficiently enhance photoactivity. The purposes of Au-doping or depositing into TiO<sub>2</sub> are: (i) to modify TiO<sub>2</sub> surface morphologies, (ii) to improve e<sup>-</sup>/h<sup>+</sup> pair's separation by acting as electron trap and, (iii) to increase the surface electron activity by localized surface plasma resonance (Sellappan et al., 2013). Au-doped TiO<sub>2</sub> catalysts, investigated for CO<sub>2</sub> photoreduction with H<sub>2</sub>O to hydrocarbons, registered higher TiO<sub>2</sub> photoactivity with Au-metal (Mei et al., 2013). Therefore, it is envisaged that gold-doped TiO<sub>2</sub> system would efficiently reduce CO<sub>2</sub> through RWGS reaction.

Among the structured supports, monolith containing parallel straight channels takes advantages of distinctive structure, higher surface area to volume ratio, and efficient light harvesting. Monolith substrate provides up to 100 times higher specific surface area than other types of catalyst supports having the same outer dimensions (Liou et al., 2011). We reported monolith photoreactor for CO<sub>2</sub> reduction and found good CO<sub>2</sub> conversion efficiency and CO selectivity (Tahir and Amin, 2015b). However, monolith photoreactor was investigated in a batch mode of operation. Recently, enhanced photocatalytic CO<sub>2</sub> reduction to CH<sub>4</sub> via steam reforming over metal-doped TiO<sub>2</sub> in a photocatalytic fluidized bed reactor has

been reported (Vaiano et al., 2015). Therefore, it is anticipated that RWGS reaction in a continuous monolith photoreactor over Au-doped TiO<sub>2</sub> would be appreciable to further enhance the photocatalysis process efficiency. The objective of this study is to test the performance of a continuous monolith photoreactor and photoactivity of Au-doped TiO<sub>2</sub> nanoparticles for the reduction of CO<sub>2</sub> by H<sub>2</sub> through RWGS reaction.

## 2. Experimental

### 2.1 Catalyst preparation and characterization

The gold-doped TiO<sub>2</sub> catalysts were synthesized using modified sol-gel method as reported previously (Tahir and Amin, 2015a). Typically, a mixture of 7 mL acetic acid and 10 mL isopropanol was added to a mixture of 10 mL titanium tetra isopropoxide in 30 mL isopropanol under vigorous stirring. The stirring was continued for 24 h until a clear sol was produced. Next, calculated amount of gold chloride (HAuCl<sub>4</sub>·3H<sub>2</sub>O), dissolved in isopropanol, was added to the titanium solution and stirred for the next 6h until clear and thick sol was obtained. The monoliths were dip-coated in the resulting Au/TiO<sub>2</sub> sol for a few seconds and excess sol was blown off using compressed hot air. The Au/TiO<sub>2</sub> monoliths and the remaining sol were dried at 80 °C for 12 h and finally calcined at a rate of 5 °C min<sup>-1</sup> up to 500 °C and held for 5 h. Similarly, TiO<sub>2</sub> samples were prepared using the same procedure.

Powder X-ray diffraction (XRD) was performed on Bruker D8 advance diffractometer. Cu- K $\alpha$  radiation was used, operating at 40 kV and 40 mA with a scan range of 10-80 degree (2 $\theta$ ), a scan speed of 1.2 degree (2 $\theta$ ) per min and wavelength ( $\lambda$ ) of 1.54Å<sup>o</sup>. The morphology of the nanocatalysts was estimated using scanning electron microscopy (SEM) carried out with JEOL JSM6390 LV SEM instrument. N<sub>2</sub> adsorption-desorption isotherms was performed at -196 °C using a Micrometrics ASAP 2020 Surface Area and Porosity Analyser. Ultraviolet-Visible (UV-Vis) diffuse reflectance absorbance spectra of the samples were determined using Agilent, Cary 100 UV-Vis spectrophotometer equipped with an integrated sphere.

### 2.2 Photoactivity test

The photocatalytic CO<sub>2</sub> reduction with H<sub>2</sub> as a reducing agent was conducted in a cylindrical stainless steel reactor of continuous flow with a total volume of 150 cm<sup>3</sup> as depicted in Figure 1 (a). The chamber was equipped with a quartz window for passing light irradiations from the reflector lamp. The catalyst coated ceramic monoliths with channels per square inch (CPSI) 200 were inserted in the middle of the chamber. The light source used was a 200 W Hg lamp for UV irradiation source. The light intensity of 150 mW cm<sup>-2</sup> was measured with an online optical process monitor ILT OPM-1D and a SED008/W sensor. All the experiments were carried out in a continuous mode using different flow rates at fixed CO<sub>2</sub>/H<sub>2</sub> molar feed ratios of 1.0. The compressed CO<sub>2</sub> and H<sub>2</sub> flow rates were regulated by mass flow controllers (MFC). The products were analyzed using an on-line gas chromatograph (GC-Agilent Technologies 6890 N, USA) equipped with a thermal conductivity detector (TCD) and a flame ionized detector (FID).

## 3. Results and discussion

### 3.1 Catalyst characterization

The XRD spectra of TiO<sub>2</sub> and Au-doped TiO<sub>2</sub> samples are presented in Figure 1 (b). The XRD peaks of pure TiO<sub>2</sub> and Au-doped TiO<sub>2</sub> revealed a pure crystalline and anatase phase TiO<sub>2</sub>. The peaks pertaining to Au-doping into TiO<sub>2</sub> were not detected. In the case of 0.3 wt. % Au, the TiO<sub>2</sub> crystallite size slightly decreased but has no significant effect in 0.5% Au-loaded TiO<sub>2</sub> (Table 1). This revealed a value of around 17±1 nm was found for all the samples with no appropriate change with the introduction of gold. Similar observations are reported previously (Hidalgo et al., 2011). The SEM images of the nanoparticles catalyst and coated over the monolith channels are presented in Figure 2. The morphology of the catalyst coated monolith is shown in Figure 2 (a-b). It is obvious that the catalyst was entirely coated over the channel surface with no broken layer observed. The TiO<sub>2</sub> nanoparticles are obvious in Figure 2 (c), identified as spherical and mesoporous TiO<sub>2</sub> structure. Similarly, Au-doped TiO<sub>2</sub> nanoparticles are shown in Figure 2 (d). Obviously, gold-doped TiO<sub>2</sub> nanoparticles are uniform in size with higher mesoporosity.

Figure 3 (a) exhibits the N<sub>2</sub> adsorption-desorption isotherms of TiO<sub>2</sub> and Au-doped TiO<sub>2</sub> nanoparticles. All the isotherms have close resemblance with type IV curve with obvious hysteresis loops, thus conforming TiO<sub>2</sub> and Au-doped TiO<sub>2</sub> as mesoporous materials. The monolayer-multilayer adsorption on the internal surface is obvious in the initial part of the isotherms (at low P/P<sub>0</sub>). The capillary condensation could be seen in the upper part of isotherms at higher P/P<sub>0</sub>, where the steep increment in the adsorption volume is observed as the pores were saturated with the liquid. (Tahir and Amin, 2015a). The specific surface area, pore volume and pore sizes of all the samples are reported in Table 1. The BET surface area of TiO<sub>2</sub> was

43 m<sup>2</sup>/g closer to BET surface area of Au-doped TiO<sub>2</sub>. Thus in the case of Au-doped-TiO<sub>2</sub> samples, the increase in the surface area was not significant. It is evident that Au-doping in TiO<sub>2</sub> samples could not alter the BET surface area, confirming no significant effect on TiO<sub>2</sub> morphology. However, the larger BJH surface area of all the Au-doped TiO<sub>2</sub> samples are attributed to the suppression of TiO<sub>2</sub> crystal growth by Au-doping, thus enhancing mesoporosity. Similarly, BJH adsorption pore volume increased with Au-doping. Thus, the increased in the BJH surface area and pore volume was obviously due to the controlled crystal growth in the Au-doped TiO<sub>2</sub> samples.

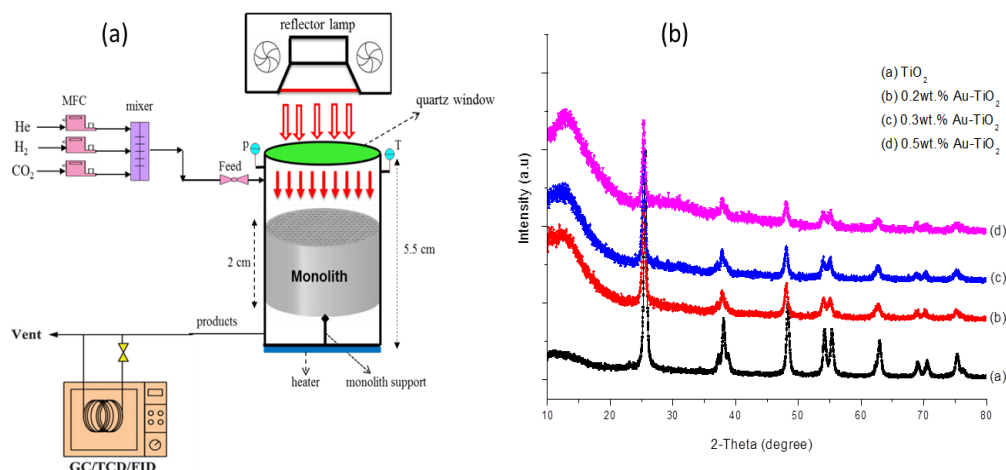


Figure 1: (a) Schematic of experimental setup for CO<sub>2</sub> reduction with H<sub>2</sub> in monolith photoreactor, (b) XRD spectra of pure TiO<sub>2</sub> and Au-doped TiO<sub>2</sub> samples with different metals concentrations

The optical properties of the pure TiO<sub>2</sub> and Au-doped TiO<sub>2</sub> were studied by measuring the absorbance spectra of wavelengths ranging from 200 to 800 nm as presented in Figure 3 (b). All the samples of Au-doped TiO<sub>2</sub> show higher absorbance intensities than un-doped TiO<sub>2</sub>. The presence of Au metal improves the absorbance spectra towards visible light due to their optical absorption spectrum ranging between 500 to 700 nm, associated with surface plasmon resonance absorption peak of Au-metal. These results confirmed that the Au-metal could enhance TiO<sub>2</sub> photoactivity in the visible region due to plasmonic response. The band gap energies were determined using Tauc plot i.e. (ahv)<sup>2</sup> versus (hv) by extrapolating the linear region of the plot to the intercept of the photon energy axis. The obtained band energy values of TiO<sub>2</sub> and Au-doped TiO<sub>2</sub> catalysts are reported in Table 1. The band gap energy of pure TiO<sub>2</sub> was 3.12 eV, reduced to 3.03 and 2.93 eV for 0.3 and 0.5 wt. % Au-doped TiO<sub>2</sub> samples, respectively. This shows Au impurity level is beneficial for extending the absorption spectrum wavelength towards the visible region.

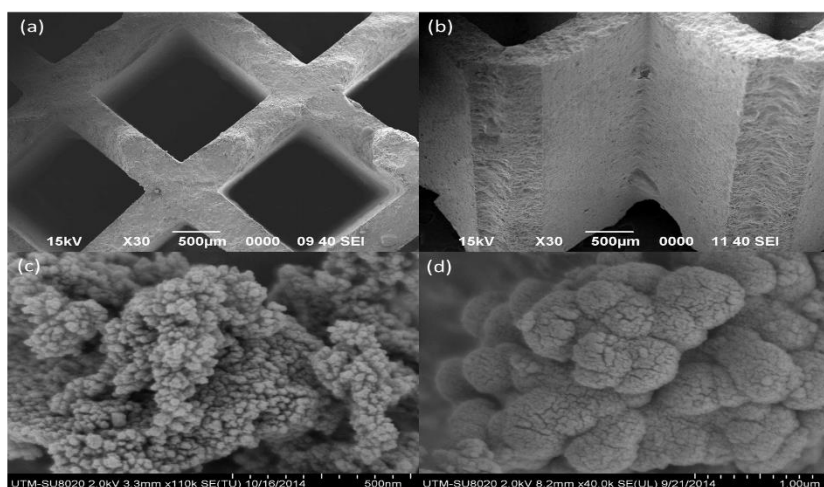


Figure 2: SEM images of TiO<sub>2</sub> and Au-doped TiO<sub>2</sub> coated over monolith channels: (a-b) front and cross section of monolith channels coated with catalysts, (c) TiO<sub>2</sub> nanoparticles (d) Au/TiO<sub>2</sub> nanoparticles.

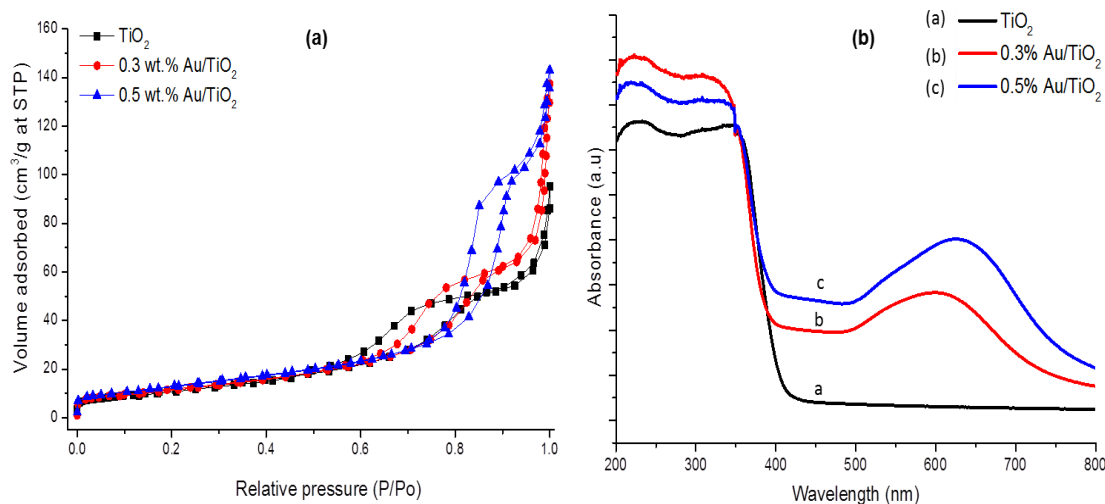


Figure 3: (a) N<sub>2</sub> adsorption-desorption isotherms of TiO<sub>2</sub> and Au-doped TiO<sub>2</sub> samples, (b) UV-Vis diffuse reflectance absorbance spectra of TiO<sub>2</sub> and Au-doped TiO<sub>2</sub> samples.

Table 1: Summary of physiochemical characteristics of TiO<sub>2</sub> and Au/TiO<sub>2</sub> samples

Catalysts	BET surface area (m <sup>2</sup> /g)	BJH adsorption surface area (m <sup>2</sup> /g)	BJH pore volume (cm <sup>3</sup> /g)	Crystallite size (nm)	Band gap energy (eV)
TiO <sub>2</sub>	43	52	0.134	19	3.12
0.3 wt.% Au- TiO <sub>2</sub>	46	58	0.23	17	3.03
0.5 wt.% Au-TiO <sub>2</sub>	47	74	0.24	18	2.93

### 3.2 Photoactivity test of CO<sub>2</sub> reduction with H<sub>2</sub>

Preliminary investigations of CO<sub>2</sub> photo-reduction with H<sub>2</sub> was performed in a continuous flow monolith photoreactor at 100 °C and feed flow rate 20 mL/min. The carbon containing compounds was not detected in the cases of (a) catalyst coated monolith without reactants under UV-irradiation, (b) reactants with catalyst coated monoliths without UV-irradiation. This confirmed catalysts and monoliths did not degrade and any carbon containing compounds produced were derived from CO<sub>2</sub> through photocatalysis.

The effects of Au-loading into TiO<sub>2</sub> for photocatalytic CO<sub>2</sub> reduction with H<sub>2</sub> to CO through RWGS reaction using different irradiation times at 100 °C, CO<sub>2</sub>/H<sub>2</sub> ratio 1.0 and flow rate 20 mL/min are presented in Figure 4 (a). At the start of the reaction, the photocatalytic CO<sub>2</sub> reduction into CO was significantly higher in all Au-doped TiO<sub>2</sub> catalysts. The maximum CO production was observed initially and then gradually reduced over the irradiation time. Using un-doped TiO<sub>2</sub> poor photoactivity is registered attributed to higher electron-hole pair's recombination rate over the TiO<sub>2</sub> surface. By doping Au-metal into TiO<sub>2</sub>, there was a substantial increase in CO<sub>2</sub> reduction to CO as the major reduction product. A 0.5 wt. % Au-doped TiO<sub>2</sub> catalyst was optimum, then the yield rates gradually decreased with higher Au-doping. The maximum production of CO over 0.5 wt. % Au-doped TiO<sub>2</sub> was 12,305 ppm g-catal.<sup>-1</sup> h<sup>-1</sup>, 318 times higher than un-doped TiO<sub>2</sub> catalysts calculated based on 2h irradiation time. Significantly higher TiO<sub>2</sub> photoactivity in the presence of Au-metal was obviously due to the plasmonic effects with hindered recombination of charges over the Au-doped TiO<sub>2</sub> surface and efficient light distribution inside monolith channels. Furthermore, in continuous monolith photoreactor, there were efficient adsorption-desorption processes, more production of electron-hole (e<sup>-</sup>/h<sup>+</sup>) pairs and their mobility over Au-doped TiO<sub>2</sub> catalysts, resulting in much higher CO production. This development confirmed higher performance of monolith photoreactor in continuous flow over Au-doped TiO<sub>2</sub> catalysts.

Among the hydrocarbons, CH<sub>4</sub> was found to be the major product in continuous monolith photoreactor at different irradiation time (0-10 h) as presented in Figure 4 (b). Using lower Au-doped TiO<sub>2</sub>, higher CH<sub>4</sub> yield rate was observed, and then gradually decreased at more Au-loading. Besides, initially, CH<sub>4</sub> yield increased and then decreased at an elongated irradiation time until reaching to steady state. The decreased in CH<sub>4</sub> production by the irradiation time was probably due to the following: Firstly, when the reaction start-up, there was higher photoactivity of catalysts, thus more production of electrons, resulting in

higher CO<sub>2</sub> photoreduction to CH<sub>4</sub>. At prolonged irradiation times, CH<sub>4</sub> production decreased, possibly due to decrease in catalyst photoactivity. Secondly, at the start-up of reaction time, there was adsorbed CO<sub>2</sub> and H<sub>2</sub>, which efficiently converted to CO and CH<sub>4</sub> in the presence of higher mobility of electrons. However, at a prolonged reaction time, there was the efficient desorption of CO with the feed stream, resulting lower possibility of its conversion to CH<sub>4</sub>. Third possibility may be the photo-oxidation of CH<sub>4</sub> with oxygen at a prolonged irradiation time in the presence of efficient monolithic catalysts, resulting in decreased of CH<sub>4</sub> production. However, the further investigation is required to find out the actual possibly way in the reduction of CH<sub>4</sub> production. The hydrocarbon products observed were C<sub>2</sub>H<sub>4</sub>, C<sub>2</sub>H<sub>6</sub>, C<sub>3</sub>H<sub>6</sub> and C<sub>3</sub>H<sub>8</sub>. The production of higher hydrocarbons confirmed higher performance of Au-doped TiO<sub>2</sub> monolithic catalysts compared to un-doped TiO<sub>2</sub>.

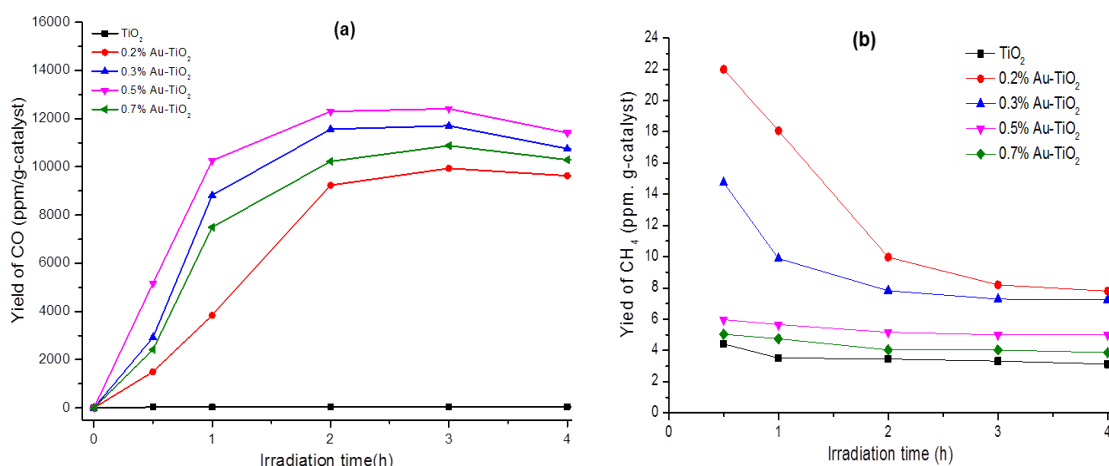


Figure 4: Effects of Au-loading and irradiation time on CO<sub>2</sub> reduction with H<sub>2</sub> at CO<sub>2</sub>/H<sub>2</sub> ratio 1.0, molar flow rate 20 mL/min, and temperature 100 °C; (a) CO production, (b) CH<sub>4</sub> production.

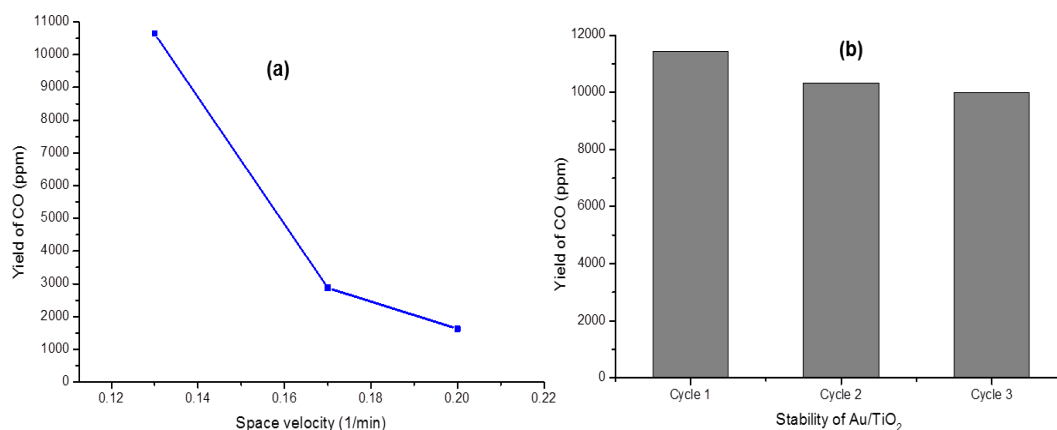


Figure 5: (a) Effects of space velocity on CO<sub>2</sub> reduction to CO at CO<sub>2</sub>/H<sub>2</sub> ratio 1.0; (b) Stability test of reused Au/TiO<sub>2</sub> for CO<sub>2</sub> reduction with H<sub>2</sub> to CO at 100 °C, CO<sub>2</sub>/H<sub>2</sub> ratio 1.0 and flow rate 20 mL/min.

The effects of space velocity on the performance of Au-doped TiO<sub>2</sub> catalyst for photocatalytic CO<sub>2</sub> reduction with H<sub>2</sub> in a monolith photoreactor are presented in Figure 5 (a). The reactant feed rates were changed to vary the space velocity at fixed CO<sub>2</sub>/H<sub>2</sub> molar ratio and keeping all other parameters constant. With the increase in space velocity, production of CO and hydrocarbons gradually decreased. It indicates, at the same reaction conditions, a lower space velocity results in higher CO<sub>2</sub> photoreduction. This is because a lower space velocity gives the reactant gases longer residence time over the catalyst surface in a monolith photoreactor (Tahir et al., 2015). In order to examine the stability of the photocatalyst,

experiments were repeated for certain times on the recycled catalyst coated monoliths. After each cycle, the monolith was removed from the reactor and placed in open air for 24 h before starting the next run. The stability test for photocatalytic CO<sub>2</sub> reduction with H<sub>2</sub> over Au-doped TiO<sub>2</sub> catalyst is illustrated in Figure 5 (b). It is noticeable CO yield was higher in the first run; gradually decreased in the second photocatalytic cyclic run, but a slight decrease in CO yield was observed after third run. Therefore, the Au-doped TiO<sub>2</sub> catalyst partially lost its activity in cyclic runs for photocatalytic CO<sub>2</sub> reduction with H<sub>2</sub> to CO. In the case of hydrocarbons, in first cyclic run, catalyst exhibits much higher CH<sub>4</sub> yield which gradually decreased in second and third cyclic runs. This was possibly catalyst lost partial photoactivity for CH<sub>4</sub> productions as explained previously. Similarly, hydrocarbons production also decreases after every run, confirming no coke production over the catalyst surface. These results exhibited better initial activity of Au-doped TiO<sub>2</sub> for the production of CH<sub>4</sub> and hydrocarbons. The colour of Au-doped catalyst during photocatalytic CO<sub>2</sub> reduction remained un-changed during every cyclic run when catalyst coated monolith was exposed to open air. These results confirmed higher stability of Au-doped TiO<sub>2</sub> catalyst, with suppressed coke production.

#### 4. Conclusions

The performance of monolith photoreactor is tested for continuous CO<sub>2</sub> reduction through RWGS reaction over Au/TiO<sub>2</sub> catalyst. CO was observed as the main product with yield rate 12,305 ppm g-catal.<sup>-1</sup> hr<sup>-1</sup>, a 318 times higher than TiO<sub>2</sub> with selectivity 99.5 % over 0.5 wt. % Au/TiO<sub>2</sub>. The higher efficiency of the monolith photoreactor was obviously due to a larger illuminated surface area, higher photon energy consumption and better utilization of reactor volume. The stability test revealed higher stability of Au-doped TiO<sub>2</sub> catalyst. Therefore, a new monolith photoreactor design is feasible in the photocatalytic reactor research field while Au-doped TiO<sub>2</sub> is a highly efficient catalyst for maximizing CO yield rates and selectivity through RWGS reaction.

#### Acknowledgements

This research work was carried out under FRGS (Fundamental Research Grant Scheme, Vot 4F404).

#### References

- Hidalgo M.C., Murcia J.J., Navío J.A., Colón G., 2011, Photodeposition of gold on titanium dioxide for photocatalytic phenol oxidation, *Applied Catalysis A: General*, 397 (1-2), 112-120.
- Inoue T., Fujishima A., Satoshi K., Honda K. 1979. Photoelectrocatalytic reduction of carbon dioxide in aqueous suspensions of semiconductor powders, *Nature*, 277, 637-638.
- Liou P.-Y., Chen S.-C., Wu J.C.S., Liu D., Mackintosh S., Maroto-Valer M., Linforth R., 2011, Photocatalytic CO<sub>2</sub> reduction using an internally illuminated monolith photoreactor, *Energy and Environmental Science*, 4 (4), 1487-1494.
- Mei B., Pougin A., Strunk J., 2013, Influence of photodeposited gold nanoparticles on the photocatalytic activity of titanate species in the reduction of CO<sub>2</sub> to hydrocarbons, *Journal of Catalysis*, 306, 184-189.
- Ruzmanova Y., Ustundas M., Stoller M., Chianese A., 2013, Photocatalytic treatment of olive mill wastewater by N-doped titanium dioxide nanoparticles under visible light, *Chemical Engineering Transactions*, 32, 2233-2238.
- Saccoa O., Vaiano V., Hanb C., Sannino D., Dionysiou D.D., Ciambella P., 2015, Long afterglow green phosphors functionalized with Fe-N doped TiO<sub>2</sub> for the photocatalytic removal of emerging contaminants. *Chemical Engineering Transactions*, 43, 2107-2112.
- Sellappan R., Nielsen M.G., González-Posada F., Vesborg P.C.K., Chorkendorff I., Chakarov D. 2013, Effects of plasmon excitation on photocatalytic activity of Ag/TiO<sub>2</sub> and Au/TiO<sub>2</sub> nanocomposites, *Journal of Catalysis*, 307, 214-221.
- Tahir B., Tahir M., Amin N.S., 2015, Performance analysis of monolith photoreactor for CO<sub>2</sub> reduction with H<sub>2</sub>, *Energy Conversion and Management*, 90 (0), 272-281.
- Tahir M., Amin N.S., 2015a, Indium-doped TiO<sub>2</sub> nanoparticles for photocatalytic CO<sub>2</sub> reduction with H<sub>2</sub>O vapors to CH<sub>4</sub>, *Applied Catalysis B: Environmental*, 162, 98-109.
- Tahir M., Amin N.S., 2015b, Photocatalytic CO<sub>2</sub> reduction with H<sub>2</sub> as reductant over copper and indium co-doped TiO<sub>2</sub> nanocatalysts in a monolith photoreactor, *Applied Catalysis A: General*, 493, 90-102.
- Vaiano V., Sannino D., Ciambella P., 2015, Steam reduction of CO<sub>2</sub> in a photocatalytic fluidized bed reactor. *Chemical Engineering Transactions*, 43, 1003-1008.
- Wang Z., Teramura K., Hosokawa S., Tanaka T., 2015, Photocatalytic conversion of CO<sub>2</sub> in water over Ag-modified La<sub>2</sub>Ti<sub>2</sub>O<sub>7</sub>, *Applied Catalysis B: Environmental*, 163, 241-247.